



Cite this: *Green Chem.*, 2018, 20, 1199

Received 12th December 2017,  
 Accepted 6th February 2018

DOI: 10.1039/c7gc03735j

rsc.li/greenchem

## An intensified atmospheric plasma-based process for the isolation of the chitin biopolymer from waste crustacean biomass†

M. Borić, <sup>a,b</sup> H. Puliyalil, <sup>a</sup> U. Novak <sup>\*a</sup> and B. Likozar<sup>a</sup>

**Atmospheric-pressure dielectric barrier discharge plasma was used as a methodology for a crustacean shell waste pre-treatment process, resulting in intensified protein removal. This renewable electricity-based separation operation can serve as a scalable green alternative to the conventional chemical purification in the production of the chitin biopolymer, which applies unrecyclable mineral bases.**

Over 10 million tons of shrimps are collected every year from the sea worldwide while 50% of their total body mass remains as waste after the utilization in the food industry.<sup>1</sup> Shrimp shell waste consists of proteins (30–40%), calcium carbonate (30–50%), chitin (20–30%) and pigments (astaxanthin, canthaxanthin, lutein or  $\beta$ -carotene)<sup>2</sup> and the production of chitin is the best way to utilize this biomass.

Chitin, a polysaccharide consisting of acetyl-glucosamine and *N*-acetyl-glucosamine monomer units, is a bio-renewable, biocompatible, environmentally friendly, biodegradable and bio-functional polysaccharide. It is easily functionalized and as such has been used for various applications in the biomedical, pharmaceutical, tissue engineering, cosmetics, and wastewater treatment sectors.<sup>3–6</sup> For chitin as a by-product of the crustacean processing industry to be of use, the removal of minerals (demineralization), proteins (deproteinization), and pigments (decolourization) is required.<sup>7</sup> For the development of efficient procedures for chitin extraction from shrimp waste, it is important to understand the structural features of the shrimp shell (exoskeleton). The crustacean exoskeleton is very rigid and it is made out of a 3-layered cuticle. Predominantly, chitin is located in the inner layers of the cuticle of the shell, wrapped together with proteins, which assist with the sclerotization of the shell. The middle layer consists of chitin with minerals while the outer layers of the cuticle are made of

calcium carbonate and proteins.<sup>8</sup> Thus for the successful isolation of chitin, exfoliation of the outer and middle layers is necessary. The conventional process for chitin recovery and purification from crustacean shells requires the use of strong alkali and acid solutions and relatively high temperatures.<sup>9,10</sup>

Due to the large amount of acidic, alkaline and organic waste generated during the process, this process is also environmentally hazardous and the effluent treatment of acid and alkaline reagents adds additional cost.<sup>11</sup> Furthermore, the continuous hydrolysis of the polymer during alkaline treatment causes a decrease in the molecular weight of chitin and therefore affects its mechanical properties.<sup>12</sup>

Thus, some commercially available crude enzymes for the chitin extraction process could be of interest in decreasing costs of this process as well as in preserving the environment. However, it must be noted that the efficiency of enzymatic methods is inferior to chemical methods with approximately 5%–10% residual protein typically still associated with the isolated chitin.<sup>12</sup> As an alternative, researchers investigated new technologies and one of the most prospective is the lactic-acid fermentation process for chitin isolation, where a mixture of bacteria consume proteins and degrade calcium carbonate. However, the process time for the completion of this fermentation step is relatively high, of the order of a few hours or days.<sup>13,14</sup> The combination of enzymatic deproteinization and lactic acid demineralization with microwave radiation under eco-friendly conditions was also proposed as an option.<sup>15</sup> Another attractive way for chitin isolation is the use of ionic liquids which dissolve chitin, leaving proteins and minerals undissolved.<sup>16</sup> A major drawback of this method is a higher cost associated with the complete recovery of the ionic liquids (recycling of the solvents).

Due to these facts, the development of efficient and greener routes for the removal of protein from crustacean shell waste remains a challenge. Lately, non-equilibrium plasmas have attracted great interest, especially for the precise and efficient surface modification of various heat-sensitive materials such as polymers or polymer composites, without affecting the bulk properties.<sup>17,18</sup> Plasma surface modifications have already

<sup>a</sup>National Institute of Chemistry, Hajdrihova 19, 1000 Ljubljana, Slovenia.  
 E-mail: uros.novak@ki.si

<sup>b</sup>Faculty of Technology and Metallurgy, Karnegijeva 4, 11000 Belgrade, Serbia

† Electronic supplementary information (ESI) available. See DOI: 10.1039/c7gc03735j



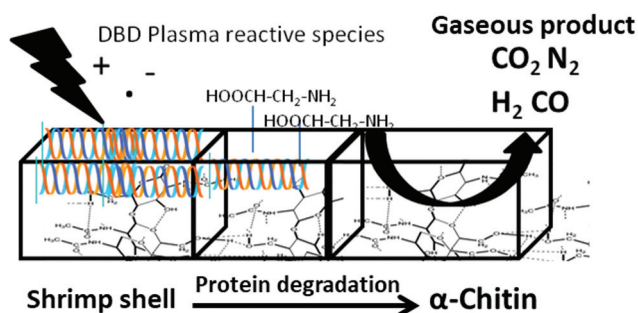
been used for the surface modification of biopolymers such as chitin or chitosan with the purpose of improving their physical and chemical characteristics for various applications.<sup>19–21</sup> Furthermore, it is well known that various gas plasma treatments are used for the degradation of human tissues, blood proteins and microorganisms as an efficient technique for sterilizing surgical devices.<sup>22</sup> Plasma generation by the dielectric barrier discharge (DBD) method provides thermally non-equilibrium plasmas (low temperature plasmas or cold plasmas) with a much higher electron temperature compared to that of ions.<sup>23</sup>

Herein, we present the method of DBD plasma assisted faster removal of outer layers from the surface of shrimp shell waste, forming gaseous products (Scheme 1). Several plasma gas compositions have been tested and extensive surface characterization (XPS, FT-IR and SEM) on the treated shrimp shell surface was performed. Furthermore, DBD plasma is a potential scalable, efficient and sustainable pre-treatment method for the removal of low value added compounds, while releasing only gaseous products, exposing the desirable biopolymer, chitin.

For our experiments, plasma was generated in a reactor made from a quartz tube, bearing an inner steel electrode, which was connected to a high voltage source with a frequency of 3 kHz. The outer electrode was made out of aluminum foil, wrapped around the reactor tube and connected to the ground. Shrimp shell parts [Fig. SI1A ESI†] were washed with demineralized water, dried and inserted into the gap between the electrode (in a volume of 3.1 cm<sup>3</sup>) and the quartz tube [Fig. SI2 ESI†]. The plasma was generated at a power introduced into the plasma of 20 W with pure N<sub>2</sub> and N<sub>2</sub>/O<sub>2</sub> mixtures at the inlet (5% and 10% O<sub>2</sub> in N<sub>2</sub> plasma).

The plasma generated with N<sub>2</sub> or N<sub>2</sub>/O<sub>2</sub> gas mixtures consists of various excited atomic and ionic species, excited molecules and electrons. Pure N<sub>2</sub> DBD plasmas are known to contain excited molecular, atomic and ionic species (N<sub>2</sub><sup>\*</sup>, N<sub>2</sub><sup>+</sup>, etc.), which can break various carbon–carbon or carbon–hydrogen bonds.<sup>24</sup> Additionally, the breakage of the surface bonds can yield various excited radical species such as atomic H or OH radicals. The experimental and theoretical studies on the

generation and detection of such species in various plasmas can be found elsewhere.<sup>24,25</sup> The effects of various plasma feed gas compositions on etching rates were measured in terms of percentage of mass removed from the sample and are presented in Fig. 1A. It was observed that by increasing the O<sub>2</sub> content in the feed gas mixture, the etch rate tended to increase, which is attributed to higher concentrations of excited O\* species.<sup>26</sup> It is already well established that atomic



**Scheme 1** Solvent-less DBD plasma-based removal of proteins from shrimp shell waste, exposing the  $\alpha$ -chitin biopolymer and forming only gaseous products.

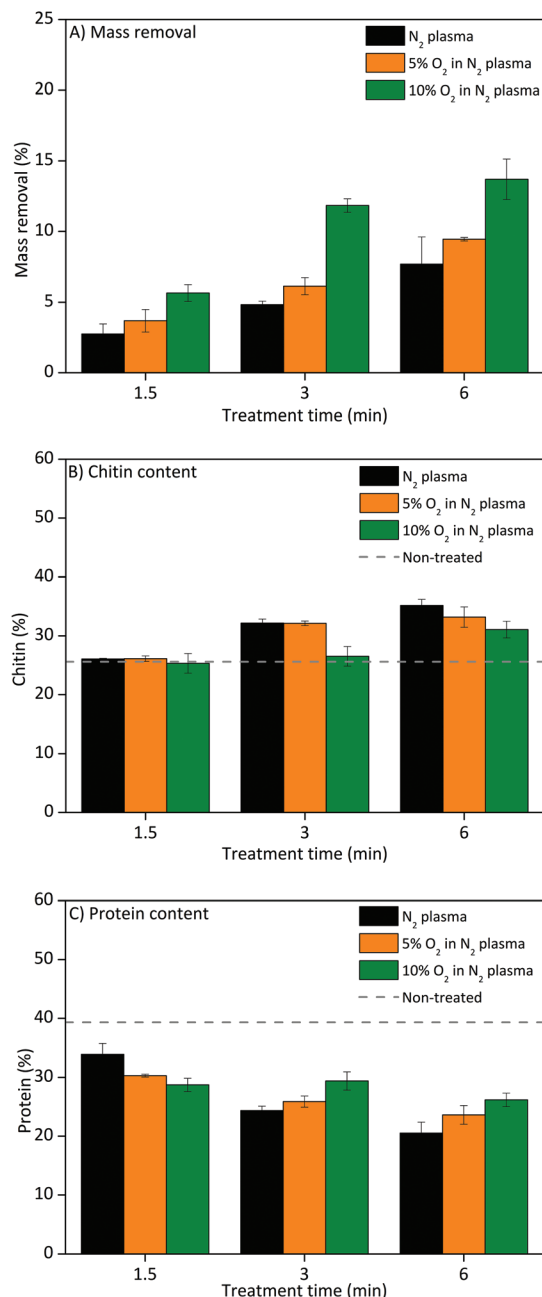


**Fig. 1** Shrimp shell treatment with N<sub>2</sub> plasma, 5% O<sub>2</sub> in N<sub>2</sub> plasma and 10% O<sub>2</sub> in N<sub>2</sub> plasma for 1.5, 3 and 6 minutes. (A) Mass removed, (B) chitin content and (C) protein content. (The composition of the non-treated shrimp shell was: chitin 25.5%, protein 37.4% and mineral (ash) content 37.1%.)



O species can react with much higher reaction kinetics with various carbonaceous materials compared to that of excited atomic or molecular nitrogen species. In order to determine the plasma selectivity towards the shrimp shell content, chitin, ash (minerals) and total nitrogen were assessed in all the samples following the protocols described in the ESI.† The protein content in waste crustacean biomass was calculated with eqn (1).

$$\text{Protein (\%)} = (\text{N}_{\text{Kjeldahl}} (\%) - \text{C}_{\text{chitin}} (\%) \cdot \text{N}_{\text{chitin}} (\%)) \cdot f \quad (1)$$

where  $\text{N}_{\text{Kjeldahl}}$  is the total nitrogen content in the sample,  $\text{C}_{\text{chitin}}$  is the chitin content in the sample,  $\text{N}_{\text{chitin}}$  is the nitrogen content in the chitin at complete acetylation (6.33%), and  $f$  is the remaining nitrogen to protein conversion factor (6.25).

Chitin concentration was estimated by completely isolating chitin from the samples following the protocol described in the ESI.†

The chitin concentration in the non-treated samples was 25.6% and was increased by 52% (37.6% in the sample) in the case of pure  $\text{N}_2$  plasma, while in the 5% and 10%  $\text{O}_2$  in  $\text{N}_2$  plasma, a lower increase in the chitin content, 42.9% (35.3% in the sample) and 34.4% (33.2% in the sample), was observed (Fig. 1B). The determination of the protein content in shrimp shells using eqn (1) showed that the protein content was decreased by 42% in the sample treated with pure  $\text{N}_2$  plasma, while with the 5%  $\text{O}_2$  and 10%  $\text{O}_2$  in  $\text{N}_2$  plasma, the values are lower, 33.7% and 26.2%, respectively (Fig. 1C). The increased values of chitin in the treated sample are in parallel with the protein removal values in the samples treated with pure  $\text{N}_2$  plasma, which makes this type of plasma less aggressive and more selective towards the outer layer of proteins. On the other hand, we assume that treatment with 5 and 10%  $\text{O}_2$  in  $\text{N}_2$  plasma also causes the decomposition of the polysaccharide chain. This behaviour of the samples treated with  $\text{O}_2$  plasma may be attributed to its more aggressive influence on the shrimp shell and the chitin chain itself. The plasma generated reactive species are removed from the shrimp shell surface layers into volatile molecules such as  $\text{CO}$ ,  $\text{CO}_2$  and  $\text{H}_2$ , which were then detected using *in-line* micro-GC measurements of the outlet gas composition. The amount of  $\text{CO}_2/\text{CO}$  and  $\text{H}_2$  released from the surface increases with the  $\text{O}_2$  content in the

inlet gas [Fig. S13, ESI†], which confirms higher material removal from the shrimp shell in that case (Fig. 1A).

During plasma treatment, the inorganic minerals were inert towards the interacting plasma reactive species. However, a slight loss of minerals was observed, which could be further explained by the chitin biopolymer matrix decomposition releasing minerals, which then additionally contribute to a higher loss of mass. Furthermore, the X-ray photoelectron spectroscopy (XPS) elemental analysis of the shrimp shell surface after plasma treatment revealed a higher mineral content in the case of 5 and 10%  $\text{O}_2$  in  $\text{N}_2$  plasma [Fig. S14, ESI†]. This could not be explained just by the removal of proteins, since the minerals in the shrimp shells are embedded in the chitin matrix, serving as a protection against mechanical damage of chitin in the bulk of the shell.<sup>8</sup> For example, when we conducted the 10%  $\text{O}_2$  in  $\text{N}_2$  plasma treatments on a demineralized sample, the sample became charred in a short time (data not shown), providing another solid argument for the mineral's protective role.

Our next objective was to study the influence of plasma treatments on surface chemistry and morphology, treated under various conditions. Since plasma is a surface sensitive technique, XPS is one of the most suitable surface analytical techniques for comparing the changes in surface chemistry before and after plasma exposure, which can collect signals from a depth of  $\sim 5$  nm. The XPS survey spectrum revealed that the surface oxygen content increased after exposure to various plasmas. Furthermore, to elucidate the surface chemistry, a high resolution C 1s peak located at around 285 eV was deconvoluted. The comparison of C 1s peaks for the samples treated with various gas plasmas is presented in Fig. 2.

The C 1s peak for the non-treated sample was deconvoluted mainly to 3 peaks. The lower binding energy peak at around 284.7 eV was assigned to C–C or C–H bond types on the surface whereas the peaks at around 286 eV and 288 eV were assigned to C–N/C–O and C=N/C=O bonds, respectively.<sup>27</sup> It should be noted that a clear distinction between carbon–nitrogen and carbon–oxygen bond types cannot be made by using XPS analysis due to their very similar binding energy values. After plasma treatment, the relative intensity of the lower binding energy peak corresponding to C–C/C–H bonds significantly decreased along with the appearance of new O–C=O bonds, confirmed by the presence of a peak above 289.5 eV.<sup>28</sup>

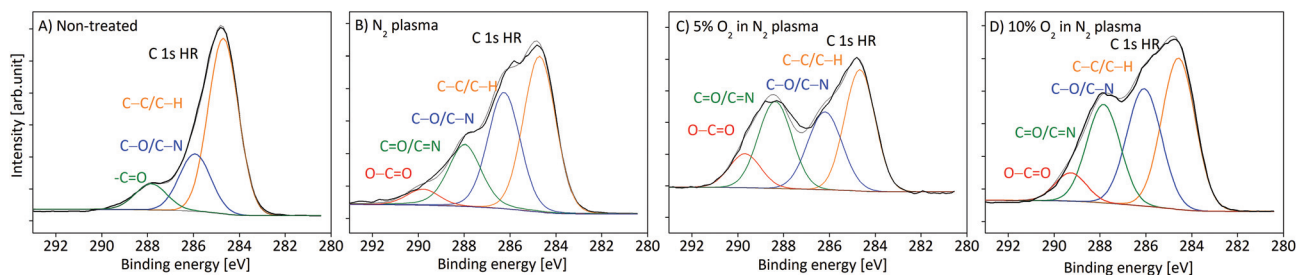
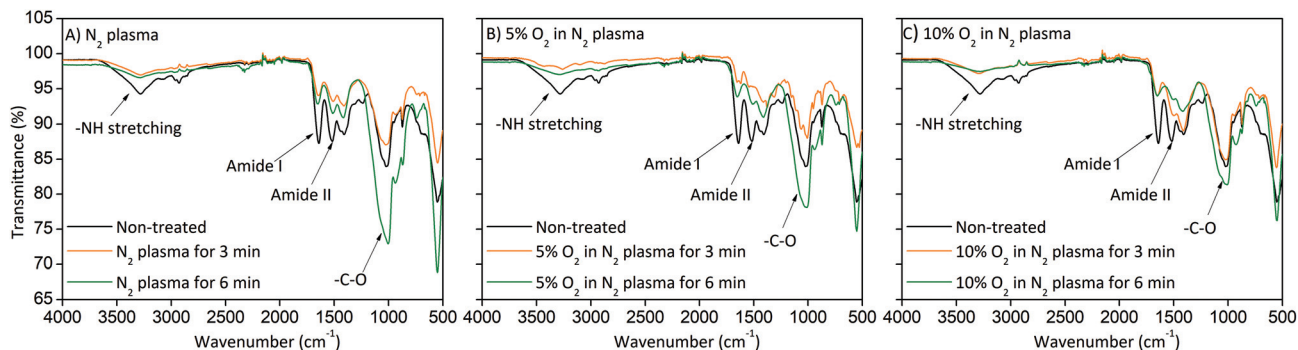


Fig. 2 XPS deconvolution of the HR C 1s spectrum for (A) the non-treated sample and the samples treated for 3 minutes with (B) pure  $\text{N}_2$  plasma, (C) 5%  $\text{O}_2$  in  $\text{N}_2$  plasma and (D) 10%  $\text{O}_2$  in  $\text{N}_2$  plasma.





**Fig. 3** FTIR spectra of the non-treated shrimp shell and shrimp shells treated for 3 and 6 minutes with (A) pure  $N_2$  plasma, (B) 5%  $O_2$  in  $N_2$  plasma and (C) 10%  $O_2$  in  $N_2$  plasma.

The relative intensities of other oxidized carbon states (peaks at 286 eV and 288 eV) were relatively higher for the samples treated with  $N_2/O_2$  mixture compared to that of the  $N_2$  plasma treated samples. This is a further confirmation of the higher carbon oxidation and increased etching rates in  $N_2$  plasma after  $O_2$  addition. Furthermore, the effects of plasma treatments were compared by using the FT-IR spectra of shrimp shells using the diamond ATR mode of operation (Fig. 3). It is already well established that the IR absorption peaks corresponding to  $-CH_3$  deformation ( $1410\text{ cm}^{-1}$ ),  $-C-O$  stretching ( $1020\text{ cm}^{-1}$ ) and  $-NH$  stretching ( $3280\text{ cm}^{-1}$ ) are characteristic peaks for chitin.<sup>29</sup>

The FT-IR spectra showed that shrimp shells after plasma treatment exhibited absorption bands at around  $3280\text{ cm}^{-1}$ ,  $1410\text{ cm}^{-1}$  and  $1020\text{ cm}^{-1}$  corresponding to  $-NH$  stretching,  $-CH_3$  deformation and  $-C-O$  stretching, respectively. All samples treated for 6 minutes showed an increase in intensity of the broad peak detected at  $1020\text{ cm}^{-1}$  due to the asymmetric vibration of  $-C-O$  of the glycosidic linkage. The samples treated for 3 minutes showed the same or lower intensity of the  $-C-O$  band, compared to the non-treated samples. Particularly in the sample treated with 5%  $O_2$  in  $N_2$  plasma for 3 minutes, a broad peak at  $1020\text{ cm}^{-1}$  in the polysaccharide region was replaced with a few distinct peaks which may be assigned to a clear form of the chitin polysaccharide chain.<sup>30</sup> On the other hand, from the protein removal point of view, the

FT-IR spectrum showed decreased intensity of bands at around  $1640\text{ cm}^{-1}$  and  $1520\text{ cm}^{-1}$  which represent amide I and amide II, respectively. The amide I band corresponds primarily to the  $C=O$  stretching vibrations and the amide II band corresponds to  $-NH$  bending. The above-mentioned bands refer to proteins and also occur in the IR spectrum of chitin because of the presence of the  $C=O$  and  $-NH$  groups in chitin. The spectra after plasma treatment showed that the intensity of a peak detected at  $1640\text{ cm}^{-1}$  was reduced (the band was broader), which indicated the removal of proteins from the sample. Also, after plasma treatment, a peak detected at  $1520\text{ cm}^{-1}$  was reduced in the samples treated with pure  $N_2$  plasma, and was absent in the samples treated with a higher concentration of oxygen, which is also a confirmation of protein removal. Also, our research provided a comparison of the FT-IR spectra of the plasma treated samples with the conventionally deproteinized samples (1 M NaOH, at  $80\text{ }^\circ\text{C}$  for 1 hour) [Fig. SI5, ESI†]. All plasma treated samples showed good matching with the deproteinized samples regarding peaks related to protein removal.<sup>31</sup>

In order to visually observe the surface changes and morphology of shrimp shells after plasma treatment and comparing them to deproteinized shrimp shells, scanning electronic microscopy (SEM) images were obtained (Fig. 4). The changes on the surface are clearly visible when compared to raw shrimp shell (Fig. 4A). The plasma treated samples exhibit

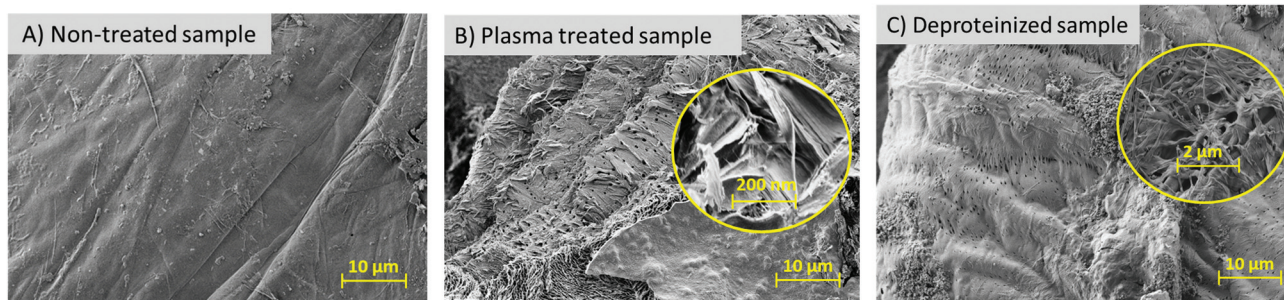


**Fig. 4** SEM images of (A) the non-treated shrimp shell, (B) the shrimp shell treated with pure  $N_2$  plasma for 6 minutes and (C) the deproteinized shrimp shell (1 M NaOH, 4 h at  $80\text{ }^\circ\text{C}$ ).



lamellar organization of fibers that form a network of strings which correlate to chitin.<sup>32</sup> A comparison of the SEM images of the N<sub>2</sub> plasma treated shrimp shell (Fig. 4B) and alkali deproteinized shell (Fig. 4C) reveals the same porous and fibrous surface on both samples. There the plasma treatment lasted only 6 min while producing only gaseous waste.

The estimated thickness of the sample before and after plasma treatment was determined using a scanning electron microscope at low electron energies. The shrimp shells before plasma treatment had an average characteristic thickness of 80 ± 10 μm, while after 10% O<sub>2</sub> in N<sub>2</sub> plasma and pure N<sub>2</sub> plasma treatment, it reduced to 35 ± 5 μm and 44 ± 8 μm, respectively. Since the typical crustacean shell composition from the outer surface to inside consists of epicuticle, exocuticle, endocuticle and inner membrane layer which could be visible as distinct layers under the SEM,<sup>33</sup> we can take into account that the outer side of the shell is more protected from the plasma influence (minerals are inert to plasma). The epicuticle consists of tanned lipoprotein impregnated with calcium salts, and the exocuticle contains chitin–protein fibers stacked in layers.<sup>33</sup> The exocuticle and endocuticle layers consist of a hard mineralized fibrous chitin–protein tissue and this section is therefore more accessible to the DBD plasma treatment, which could further explain the reduction of the thickness and exposed characteristic chitin fibrous structure (Fig. S11B ESI†). Furthermore, we have determined the characteristic thickness of the deproteinized shrimp shells and the results revealed almost the same thickness as that of the plasma treated shrimp shells (40 ± 10 μm).

Further examination of the plasma treatment on shrimp shells in combination with the consecutive removal of minerals is envisioned in the future.

## Conclusions

The establishment of a profitable and sustainable industry from shrimp shell waste is in need of new approaches. The development of a sustainable fractionation method to separate proteins, calcium carbonate and chitin, one that avoids corrosive or hazardous reagents and minimizes waste, is being envisioned as a solution.<sup>11</sup> The DBD plasma treatment process showed an efficient and fast protein removal capability without a significant influence on the chitin biopolymer. Furthermore, the plasma based process does not require any solvents and therefore no (solid and liquid) waste is formed. Using relatively cheap gaseous O<sub>2</sub>/N<sub>2</sub> mixture and working under atmospheric pressure without using any expensive vacuum components enables a straightforward scale-up of this technology. Examples can be found in the cited reference for the industrial-scale plasma processing for various commercial applications.<sup>34</sup> With this in mind, after an initial investment to build a new plasma system, the day-to-day expenses for the operation are mostly limited to the cost for electricity, which makes it even more appealing to be embraced for the chitin isolation process in the future. For complete chitin isolation,

the demineralization and complete deproteinization should be performed. However, any protocol for further isolation of the chitin from the plasma pre-treated shrimp shell should be able to isolate chitin in an intensified way saving costs on the chemicals and waste removal.

## Conflicts of interest

There are no conflicts of interest to declare.

## Acknowledgements

This work was facilitated by the Mar3Bio project, financed through the first call of the Marine Biotechnology ERA-NET (funded under the European Commission's Seventh Framework Programme), and the BioApp project (Interreg V-A Italy-Slovenia 2014–2020), its operation co-funded by the European Regional Development Fund. The authors also acknowledge the financial support from the Slovenian Research Agency (research core funding No. P2-0152), as well as Prof. Dr Janez Kovač, Dušan Komel and Ana Bjelić for XPS, Kjeldahl and SEM analyses, respectively.

## References

- 1 V. L. Pachapur, K. Guemiza, T. Rouissi, S. J. Sarma and S. K. Brar, *J. Chem. Technol. Biotechnol.*, 2016, **91**, 2331–2339.
- 2 S. A. Radzali, B. S. Baharin, R. Othman, M. Markom and R. A. Rahman, *J. Oleo Sci.*, 2014, **63**, 769–777.
- 3 X. Shen, J. L. Shamshina, P. Berton, G. Gurau and R. D. Rogers, *Green Chem.*, 2016, **18**, 53–75.
- 4 Y. Tsutsumi, H. Koga, Z. D. Qi, T. Saito and A. Isogai, *Biomacromolecules*, 2014, **15**, 4314–4319.
- 5 P. Sacco, A. Travan, M. Borgogna, S. Paoletti and E. Marsich, *J. Electron. Mater.*, 2015, **10**, 26–128.
- 6 S. Babel and T. A. Kurniawan, *J. Hazard. Mater.*, 2003, **97**, 219–243.
- 7 V. Zargar, M. Asghari and A. Dashti, *ChemBioEng Rev.*, 2015, **2**, 204–226.
- 8 F. Gagne and C. Blaise, *Comp. Biochem. Physiol., Part C: Toxicol. Pharmacol.*, 2004, **138**, 515–522.
- 9 J. Kumirska, M. Czerwicka, Z. Kaczyński, A. Bychowska, K. Brzozowski, J. Thöming and P. Stepnowski, *Mar. Drugs*, 2010, **8**, 1567–1636.
- 10 T. B. Cahú, S. D. Santos, A. Mendes, C. R. Córdula, S. F. Chavante, L. B. Carvalho, H. B. Nader and R. S. Bezerra, *Process Biochem.*, 2012, **47**, 570–577.
- 11 N. Yan and X. Chen, *Nature*, 2015, **524**, 154–157.
- 12 I. Younes and M. Rinaudo, *Mar. Drugs*, 2015, **13**(3), 1133–1174.
- 13 P. Liu, S. Liu, N. Guo, X. Mao, H. Lin, C. Xue and D. Wei, *Biochem. Eng. J.*, 2014, **91**, 10–15.



- 14 H. Zhang, Y. Jin, Y. Deng, D. Wang and Y. Zhao, *Carbohydr. Res.*, 2012, **362**, 13–20.
- 15 A. U. Valdez-Peña, J. D. Espinoza-Perez, G. C. Sandoval-Fabian, N. Balagurusamy, A. Hernandez-Rivera, I. M. De-la-Garza-Rodriguez and J. C. Contreras-Esquivel, *Food Sci. Biotechnol.*, 2010, **19**, 553–557.
- 16 Y. Qin, X. Lu, N. Sun and R. D. Rogers, *Green Chem.*, 2010, **12**, 968.
- 17 J. Delaux, M. Nigen, E. Fourré, J.-M. Tatibouët, A. Barakat, L. Atencio, J. M. García Fernández, K. De Oliveira Vigier and F. Jérôme, *Green Chem.*, 2016, **18**, 3013–3019.
- 18 H. Puliyalil, G. Filipic, J. Kovac, M. Mozetic, S. Thomas and U. Cvelbar, *RSC Adv.*, 2016, **6**, 95120–95128.
- 19 T. Vasilieva, S. A. Lopatin and V. P. Varlamov, *Carbohydr. Polym.*, 2017, **163**, 54–61.
- 20 T. M. Vasilieva, S. A. Lopatin and V. P. Varlamov, *High Energy Chem.*, 2016, **50**, 150–154.
- 21 I. Prasertsung, S. Damrongsakkul and N. Saito, *Polym. Degrad. Stab.*, 2013, **98**, 2089–2093.
- 22 X. T. Deng and J. J. Shi, *Appl. Phys. Lett.*, 2007, **90**, 013903.
- 23 S. Theapsak, A. Watthanaphanit and R. Rujiravanit, *ACS Appl. Mater. Interfaces*, 2012, **4**, 2474–2482.
- 24 Y. W. Yang, J. Y. Wu, C. T. Liu, G. C. Liao, K. Y. Cheng, M. H. Chiang and J. S. Wu, *Plasma Processes Polym.*, 2015, **12**, 678–690.
- 25 R. Dorai and M. J. Kushner, *J. Phys. D: Appl. Phys.*, 2003, **36**, 666–685.
- 26 O. Joubert, J. Pelletier and Y. Arnal, *J. Appl. Phys.*, 1989, **65**, 5096–5100.
- 27 H. Puliyalil and U. Cvelbar, *Nanomaterials*, 2016, **6**, 108.
- 28 H. Puliyalil, P. Slobodian, M. Sedlacik, R. Benlikaya, P. Riha, K. Ostrikov and U. Cvelbar, *Front. Chem. Sci. Eng.*, 2016, **10**, 265–272.
- 29 K. Prabu and E. Natarajan, *Adv. Appl. Sci. Res.*, 2012, **3**, 1870–1875.
- 30 B. A. Stankiewicz, M. Mastalerz, C. H. J. Hof and R. P. Evershed, *Org. Geochem.*, 1998, **28**, 67–76.
- 31 N. N. Kalnin, I. A. Baikalov and S. Y. Venyaminov, *Biopolymers*, 1990, **30**, 1273–1280.
- 32 M. Kaya, V. Baublys, I. Šatkauskienė, B. Akyuz, E. Bulut and V. Tubelyte, *Int. J. Biol. Macromol.*, 2015, **79**, 126–132.
- 33 Y. Xu, M. Bajaj, R. Schneider, S. L. Grage, A. S. Ulrich, J. Winter and C. Gallert, *Microb. Cell Fact.*, 2013, **12**, 90.
- 34 Plasmamatreat USA, Inc. company leaflet, (accessed January 2018) [https://www.plasmamatreat.com/downloads/english/1403\\_JOT\\_SchmitzCargobull\\_ovv\\_bsv.bri.pdf](https://www.plasmamatreat.com/downloads/english/1403_JOT_SchmitzCargobull_ovv_bsv.bri.pdf).

